Fermi National Accelerator Laboratory

FERMILAB-Conf-95/116-E
D0

Jet Shapes at D0 and CDF

Kathleen Turner Streets

Fermi National Accelerator Laboratory
P.O. Box 500, Batavia, Illinois 60510

New York University
New York, New York 10003

May 1995

Submitted for the proceedings of the *XXXth Rencontres de Moriond on QCD and High Energy Interactions*, Les Arcs, Savoie, France, March 19-26, 1995

Operated by Universities Research Association Inc. under Contract No. DE-AC02-76CHO3000 with the United States Department of Energy

Disclaimer

JET SHAPES AT DØ AND CDF

Kathleen Turner Streets
(for the DØ Collaboration)
New York University, New York, NY 10003, USA

Abstract

The distribution of the transverse energy in jets has been measured in $p\bar{p}$ collisions at $\sqrt{s} = 1.8$ TeV at the Fermilab Tevatron collider using the CDF and DØ detectors. This measurement of the jet shape is made as a function of jet transverse energy in both experiments and as a function of the jet pseudorapidity in the DØ experiment. Comparisons to Monte Carlo simulations and next-to-leading order partonic QCD calculations, $\mathcal{O}(\alpha_s^3)$, are presented.

Submitted for the proceedings of the *XXXth Rencontres de Moriond on QCD and High Energy Interactions*, Les Arcs, Savoie, France, March 19-26, 1995

Introduction

This paper describes analyses done by the DØ [1)] and CDF [2)] collaborations to determine the shapes of jets due to gluon radiation and fragmentation by measuring the radial distribution of transverse energy in jets. The dependence of the jet shape on jet transverse energy (E_T) has been measured by both collaborations. The DØ collaboration has also extended the measurement to the previously unexplored forward pseudorapidity (η) region. The data are compared to Monte Carlo and to next-to-leading order (NLO) QCD predictions at the parton level. Partonic theory of jet production at leading order, in which each jet is described by a single parton, cannot make a meaningful prediction of the jet shape. In the NLO, $\mathcal{O}(\alpha_s^3)$, calculations the jet substructure is the result of gluon radiation. Fragmentation is not included in the calculation.

Data Selection and Analysis

The detectors and jet algorithms have been described in detail elsewhere [3,4,5,6)]. During data collection, jet events were selected by requiring clusters of transverse energy in a specified number of trigger towers to exceed various thresholds. Jets were reconstructed offline using information from energy deposition in the calorimeters and the event vertex, which was determined from reconstructed tracks in the central tracking detectors. A fixed cone jet algorithm with radius, $R = \sqrt{(\Delta\eta)^2 + (\Delta\phi)^2}$, equal to 1.0 was used in the jet shape analyses. If two jets shared greater than 50% of the lower $\mathrm{E_T}$ jet's energy (75% for CDF), they were merged into a single jet, otherwise they were split into two distinct jets. The momentum of a merged jet is the vector sum of the two original jet momenta, and the energy is the sum of the two original jet energies. For split jets, the energy of each cell in the overlap region was assigned to the nearest jet and the jet directions were recalculated. The DØ jet direction is defined as $\eta_{jet} = -\ln(\tan(\theta_{jet}/2))$; $\phi_{jet} = \tan^{-1}(\sum_i E_{yi}/\sum_i E_{xi})$ where $\theta_{jet} = \tan^{-1}\sqrt{(\sum_i E_{xi})^2 + (\sum_i E_{yi})^2}/\sum_i E_{zi}$ and the transverse energy of the jet is defined as $\mathrm{E_{Tjet}} = \sum_\mathrm{i} \mathrm{E_i}\sin(\theta_\mathrm{i})$. The CDF jet direction is defined as $\eta_{jet} = \sum \eta_i E_{Ti}/\sum E_{Ti}$ and $\phi_{jet} = \sum \phi_i E_{Ti}/\sum E_{Ti}$. The sums extend over all towers (i) within the cone.

In the offline analysis, the event vertex was required to be within $\pm$ 30 cm and $\pm$ 60 cm of the detector center for DØ and CDF, respectively. To remove trigger biases, the $\mathrm{E_T}$ of the leading jet in each event was required to be above a minimum threshold. For the DØ analysis, all jets that passed quality cuts to remove spurious jets were considered and used to populate four non-overlapping jet $\mathrm{E_T}$ ranges of 45-70, 70-105, 105-140 and greater than 140 GeV. Jets were analyzed in a central region of $|\eta| \leq 0.2$ and a forward region of $2.5 \leq |\eta| \leq 3.0$. In the CDF analysis, three non-overlapping jet $\mathrm{E_T}$ samples of 40-60, 65-90, and 95-120 were used in the range $0.1 \leq |\eta| \leq 0.7$.

The jet shapes were measured by CDF using tracking information and by DØ using calorimeter information. The jet cone is divided into 10 subcones around the jet axis with radii r varying from 0.1 to 1.0 in $\Delta r = 0.1$ increments. The cumulative fraction of jet $\mathrm{E_T}$ is measured as a function of radial distance from the jet axis: $\rho(r) = \frac{1}{N_{jets}} \sum_{jets} \frac{E_T(r)}{E_T(R=1)}$ using the distance r from the jet axis of each track or calorimeter cell in the jet and the measured $\mathrm{E_T}$ ($\mathrm{P_T}$ for CDF). By definition, $\rho(r) = 1$ at $r = 1.0$. At a given value of r, $\rho(r)$ is larger for narrower jets than for broader jets.

For binning purposes, jets were corrected for the calorimeter energy scale. In CDF, the jet shape measurement was corrected for the tracking efficiency and the jet axis position resolution. The total systematic uncertainty in the CDF jet shape measurement was estimated to change the value of $\rho(r)$ by 10% to 12% over the energy ranges measured in the first subcone. This uncertainty is less than 1% for radii > 0.5. In the DØ analysis, the jet shape measurement was corrected for the underlying event and for pedestal biases resulting from zero suppression. The contribution to the jet shape due to showering in the calorimeter was removed, thereby allowing the measurement of the jet shape at the particle level. The total statistical plus systematic uncertainty in the DØ measurement was determined to be 2% to 4% in the inner subcones and decreases to less than 1% at large radii.

Preliminary Results

Figures 1 and 2 show the jet shapes measured in the central region by CDF for the three $\mathrm{E_T}$ ranges and by DØ for the four $\mathrm{E_T}$ ranges, respectively. The jet shape measurement by DØ in the forward region is shown in Fig. 3. The DØ measurement in the central region is consistent with that measured for charged particles by CDF at a comparable jet $\mathrm{E_T}$. In both the central and forward η regions, the jets narrow with increasing jet $\mathrm{E_T}$. Jets of the same $\mathrm{E_T}$ are narrower in the forward region than in the central region.

The jet shapes measured by DØ are compared to HERWIG [7)], a leading logarithm shower Monte Carlo, in Fig. 4 and Fig. 5. HERWIG describes the data well in the central region, but predicts narrower jets in the forward region.

The NLO theoretical predictions, in which there can be one or two partons in a jet, are calculated using the same $\mathrm{E_T}$ and η ranges as the data. The energy of a jet is the sum of the energies of the partons and the jet momentum is the vector sum of the momenta of the partons, using the η and ϕ definitions for CDF and DØ defined previously.

The CDF data are compared to NLO theoretical QCD predictions by Ellis, Kunzst and Soper [8)], using HMRSB pdf's and two different values of the renormalization scale, μ, in Fig. 6. There were two different parton clustering algorithms used in the prediction. The first algorithm clusters two partons into a single jet if they are each within a distance of 1.0 in

$\eta - \phi$ space of the jet direction (labelled $R_{sep} = 2$). The second algorithm requires also that they are within a distance of 1.3 of each other (labelled $R_{sep} = 1.3$). Using the $R_{sep} = 1.3$ algorithm, the prediction describes the data well; that using the $R_{sep} = 2$ algorithm is wider than the data.

The DØ data are compared in Fig. 7 and Fig. 8 to the predictions by Giele, Glover and Kosower, using JETRAD [9] with CTEQ2M pdf's and various values of the renormalization scale. Figure 7 shows the predictions with the same clustering algorithm (labelled JETRAD) as the $R_{sep} = 2$ algorithm described above. The algorithm shown in Fig. 8 (labelled JETRAD*) clusters two partons into one final state jet if they are within a distance of 1.0 of each other. The prediction using the JETRAD algorithm describes the data qualitatively in the central region but predicts much wider jets in the forward region. Using the JETRAD* algorithm, the predictions describe the data qualitatively in the forward region, but predict narrower jets in the central region. Most of the calculations predict jets in the same E_T range to be broader in the forward region than in the central region, in contrast to the data.

Conclusions

The jets in both the DØ and CDF measurements narrow as the jet E_T increases. Jets measured in the DØ analysis are narrower in the forward region than in the central region for jets with the same E_T. Because the jet shape measurement is a first order prediction at partonic NLO, large effects due to the uncertainty in the renormalization scale are expected and seen. At NLO, no single renormalization scale or parton clustering algorithm consistently describes the data in all E_T and η ranges.

We thank Walter Giele for many helpful discussions and assistance in the use of JETRAD. We thank Steve Ellis for many helpful discussions and for providing theoretical predictions.

References

(1) B. Abbott, Ph.D. thesis, Purdue University, 1994 (unpublished).
(2) CDF Collaboration, F. Abe *et al*, Phys. Rev. Lett., **70**, 713 (1993).
(3) CDF Collaboration, F. Abe *et al*, Nucl. Instrum. Methods Phys. Res., Sect. A **271**, 387 (1988).
(4) DØ collaboration, S. Abachi *et al.*, Nucl. Instrum. Methods Phys. Res., Sect. A **338**, 185 (1994).
(5) CDF Collaboration, F. Abe *et al*, Phys. Rev. D, **45**, 1448 (1992).
(6) H. Weerts, in proceedings of *9th Topical Workshop on Proton-Antiproton Collider Physics*, edited by K. Kondo and S. Kim, (Universal Academy Press, Tokyo, Japan, 1994).
(7) G. Marchesini and B.R. Webber, Nucl. Phys. **B310**, 461 (1988).
(8) S. Ellis, Z. Kunszt, D. Soper, Phys. Rev. Lett., **69**, 3615 (1992).
(9) W.T. Giele, E.W.N. Glover and D.A. Kosower, Report No. Fermilab-Pub-94/070-T, 1993.

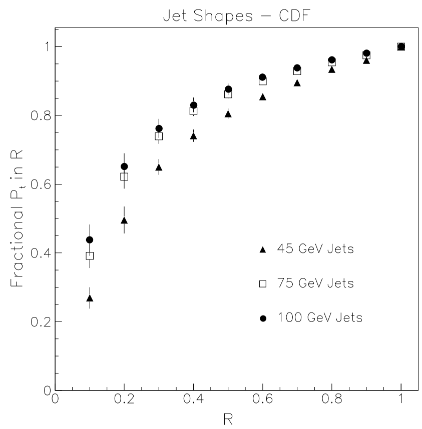

Figure 1: The distribution of the P_T fraction in a cone versus radial distance from the jet axis for $0.1 \leq |\eta| \leq 0.7$ for the three jet E_T ranges.

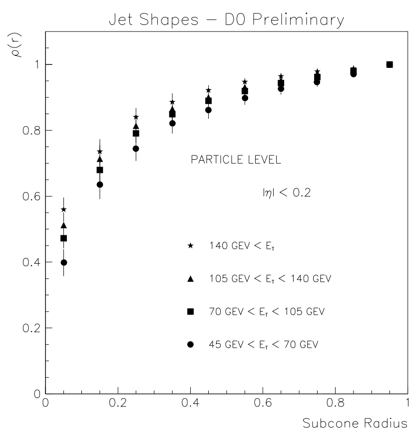

Figure 2: The distribution of the E_T fraction in a cone versus radial distance from the jet axis for central jets in the four jet E_T ranges.

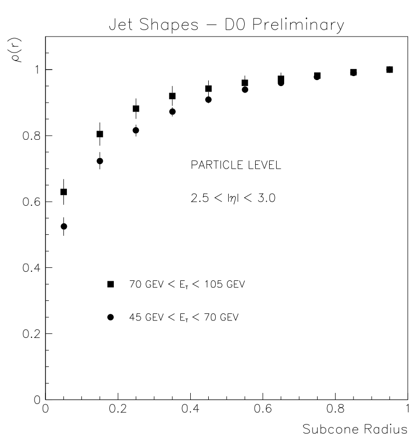

Figure 3: The distribution of the E_T fraction in a cone versus radial distance from the jet axis for forward jets in two jet E_T ranges.

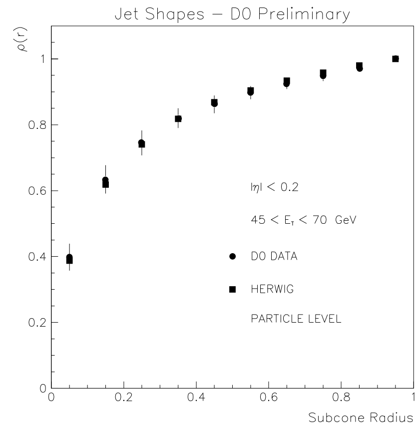

Figure 4: The DØ jet shape in the central region compared to the HERWIG Monte Carlo.

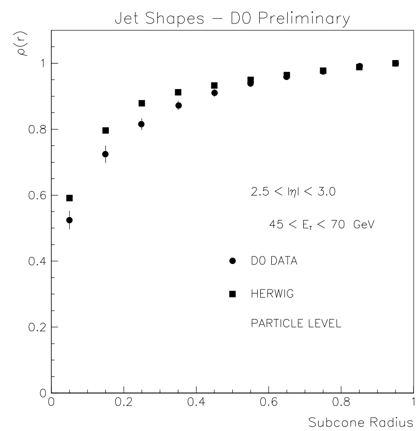

Figure 5: The DØ jet shape in the forward region compared to the HERWIG Monte Carlo.

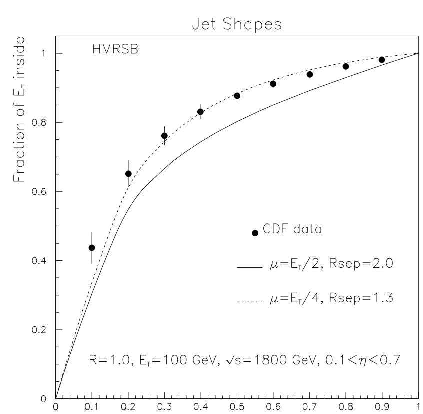

Figure 6: Comparison of the jet shape measured by CDF to a NLO prediction, using two different clustering methods and renormalization scales.

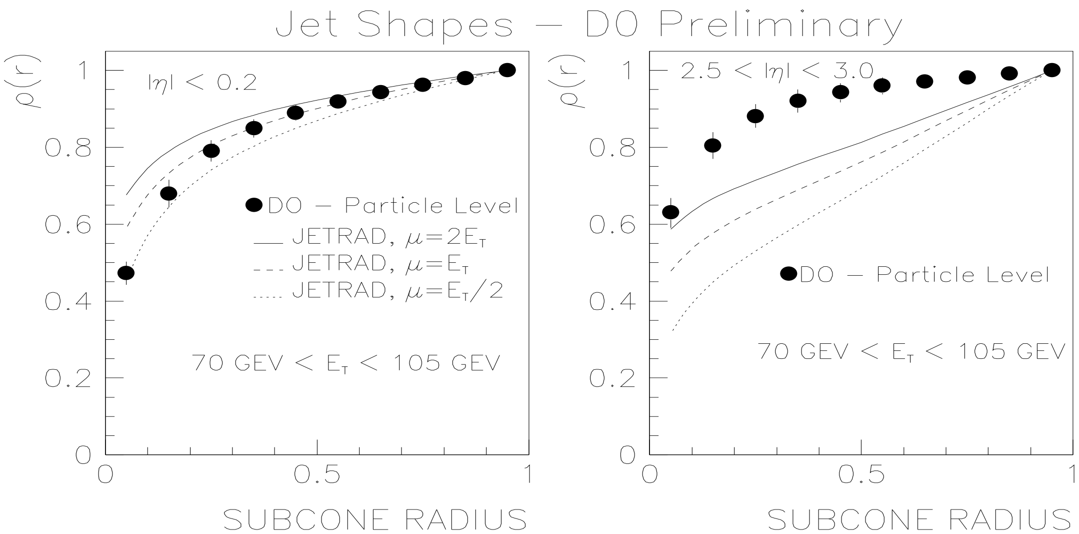

Figure 7: Comparison of the jet shapes in the central and forward regions measured by DØ to a NLO prediction using the JETRAD clustering algorithm and three different renormalization scales.

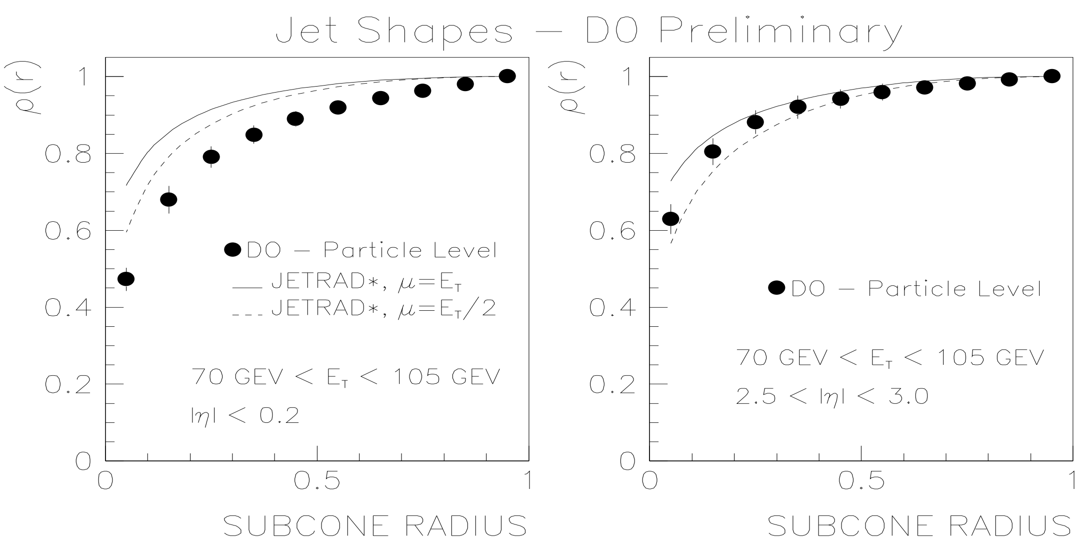

Figure 8: Comparison of the jet shapes in the central and forward regions measured by DØ to a NLO prediction using the JETRAD* clustering algorithm and two different renormalization scales.